VNU Journal of Science: Earth and Environmental Sciences

Journal homepage: https://js.vnu.edu.vn/EES

Original Article

Urban Classification Using Multi-temporal Sentinel-1 Data Based On Coherence Characteristics

Le Minh Hang[1,*], Tran Anh Tuan[2,3]

[1]*Le Quy Don Technical University, 236 Hoang Quoc Viet, Bac Tu Liem, Hanoi, Vietnam*

[2]*Institute of Ecology and Biological Resources, Vietnam Academy of Science and Technology (VAST), 18 Hoang Quoc Viet, Cau Giay, Hanoi, Vietnam*

[3]*VNU University of Science, 334 Nguyen Trai, Thanh Xuan, Hanoi, Vietnam*

Received 02 September 2020
Revised 05 October 2020; Accepted 21 October 2020

Abstract: The paper presents the method of urban classification using the coherence characteristics of pairs of SAR images observed at different times. Two scenes of Sentinel-1A VV and VH polarized on January 16, 2020, and January 28, 2020, in some central districts of Hanoi city were used experimentally in this study. The primary data processing steps included: (1) Creating the coherence image by using a pair of SAR interference images; (2) Processing coherence image by computing multi-look and geometric correction to UTM coordinate system; (3) Classification of the coherence image to urban/non-urban areas threshold method. The results showed that the urban extracted from the VH polarization image was better than the VV polarization image. The overall accuracy of classification achieved for VV and VH polarized images were 89% and 93%. Using SAR image pairs to classify urban areas that were not affected by weather conditions, showed good efficiency in managing and monitoring urban space in Vietnam cities

Keywords: Sentinel-1, coherence, urban areas, SAR image.

1. Introduction

Urban residents include building, transportation, and open space. With the increase of the population in major cities, urban land use has increased rapidly, especially in developing countries [1]. Unplanned urban growth may have a long-term negative impact on urban sustainability on a range of regional, national, and inter-governmental capabilities [2]. The

* Corresponding author.
E-mail address: leminhhang81@gmail.com

https://doi.org/10.25073/2588-1094/vnuees.4637

changes in urban land use have a significant effect on the environment and human lives. The increase in impermeable surfaces will affect these areas' drainage system, the possibility of inundation will increase, urban heat island will occur, and air pollution will increase. Hence, updating and monitoring urban land-use changes plays a vital role in planning a sustainable development city

Optical imagery is currently the primary data in land-use/land-cover classification studies, mainly urban areas classification—the urban areas are concrete and asphalt, reflecting strength in the infrared thermal bands. Therefore, many studies have used bare soil indices of the optical images such as NDBI (Normalized difference built-up index), EBBI (Enhanced built-up and Bareness index), IBI (Index-based built-up index), and NDBaI (Normalized difference bareness index) to classify urban areas [3-7]. The urban and non-urban areas on these index images often are classified by the global threshold method. The accuracy classification using bare soil indexes achieves over 80% [3-7]. However, sometimes the optical imagery is also limited as clouds and weather conditions often influence it. Therefore, microwave remote sensing data unaffected by weather conditions, day and night, are used to classify urban areas.

Sentinel-1 is a part of the European Copernicus program under the European Space Agency (ESA) domain with two SAR satellites (Sentinel-1A and Sentinel-1B) with C band and dual-polarization as VV and VH. The Sentinel-1A satellite was successfully launched into orbit in 2014 and the Sentinel-1B satellite in 2016. The revisit time is 12 days. In this article, the authors proposed to classify urban areas using the coherence maps in SAR interferometry of two Sentinel-1 images.

Many studies have proved that SAR coherence in a short period (about six days) contains information on land use/land cover (LULC), such as forest, vegetation, and urban areas [8,9]. The mean of the local coherence γ was estimated from the pair of SAR interference images' phase noise. The coherence map has value ranges from 0 to 1. The SAR coherence value has proved useful in classifying urban areas such as building and road [8]. The land-cover features have differenced coherence values in considering a period. Therefore, it is possible to classify land-cover features using multi-temporal SAR images based on the coherence and backscatter value [10,11]. Washaya et al. (2018) [12] used Coherence Change Detection (CCD) technique to monitor natural disasters in urban areas. CCD technique was proven to be suitable with the Sentinel-1 data, but multi-temporal Sentinel-1 data were used to determine coherence acquired with the same looking angle and 6 to 12 days revisit times. Besides, CCD is not suitable for a highly vegetated area [12]. Chini Marco et al. (2017) [11] proposed an automatic algorithm to map built-up areas by backscattering intensity and coherence value of the interferometric coherence images. Corbane et al. (2017) [8] compared the urban areas classification accuracy using Landsat, Sentinel-1 with Level-1 Ground Range Detected (GRD), and Sentinel-1 combined multi-temporal coherence and backscatter intensity change. The overall classification accuracy using Landsat data, Sentinel-1 GRD, and Sentinel-1 coherence is respectively 75%, 80%, and 92%. Thus, the combination with coherence information has improved the classification accuracy by using multi-temporal SAR image.

In Vietnam, many studies have used remote sensing imagery to classify urban areas. The researchers experimented with the bare soil indexes on optical satellite images to discriminate urban areas such as the NDBaI index [13], IBI index [14], EBBI [15]. The classification accuracy using these bare soil indexes with the Vietnam case study is high, over 80% [13-15]. Optical satellite image data is still the primary remote sensing data in LULC classification studies. Besides, SAR images are currently studying for many applications in Earth observation. SAR data mainly use InSAR techniques to research as DEM [16], subsidence

land [17,18], or use to classify rice [19,20]. Hang et al. (2016) [21] proposed to use backscatter intensity changes on multi-temporal Sentinel-1A images to determine land-cover features. This study proved that the backscatter of urban areas in SAR images is high and stable on multi-temporal data. It is a few studies of the coherence map in Vietnam. Therefore, the article contributes to apply Sentinel-1 images for Earth observation in Vietnam.

2. Study area and the materials

2.1. Study area

Hanoi locates in the Northern of Vietnam, in Vietnam's Red River delta (Fig. 1a). Hanoi is the second-largest city in Vietnam, with over eight million residents within the town proper and an estimated 20 million population within the metropolitan area. The selected study area includes districts of Phuc Tho, Thach That, Quoc Oai, Chuong My, Thanh Oai, Ha Dong, Hoai Duc, Tu Liem, and Dan Phuong (Fig. 1b, 1c). This area has urbanization dramatically. There are many types of land-use/land-cover (LULC), such as vegetation (urban green trees, rice, crops, shrub), open water (lake, river), and urban areas (building, barren land, roads). The topography of the site is relatively flat, with no hills or high mountains.

2.2. Materials

The material data used are two Sentinel-1A images acquired on 16/01/2020 and 28/01/2020 with the same track, in which the characteristics are shown in Table 1.

The level processing of the image is Level-1 Single Look Complex (SLC) products. Each image pixel in the SLC product is represented by a complex (i and q) magnitude value with 16 bits per pixel. The pixel spacing was determined in azimuth by the pulse repetition frequency (PRF) and in range by the radar range sampling frequency. SLC products were processed as a single look in each dimension by using the full available signal bandwidth. The imagery was geo-referenced using orbit and attitude data from the satellite. The SLC product contains three sub-swaths, such as IW1, IW2, and IW3, and each sub-swath has dual-polarization VV and VH.

In this study, the authors used sub-swath IW2 with two polarizations VV and VH, to determine the coherence map. Table 1 shows that Sentinel-1A pair images include a perpendicular baseline -12.6m, the high modeled coherence value 0.98. Hence, two Sentinel-1A images are suitable for using the InSAR technique and determining the coherence map.

Table 1. The characteristic of the experience data

Parameters	Description	
	16/01/2020 (Master)	28/01/2020 (Slave)
Product type	Sentinel-1A with (SLC/IW) Level-1	
Track number	128	128
Pass	Ascending	
Central incidence angle	21.289394386 (lat)	21.289381512 (lat)
	105.288348029 (lon)	105.288394006 (lon)
Slant range resolution (m)	2.329562	2.329562
Azimuth resolution (m)	13.97952	13.97952
Polarization	VV and VH	
Perpendicular Baseline	-12.6	
Modeled Coherence	0.98	
Orbit number	30825	31000

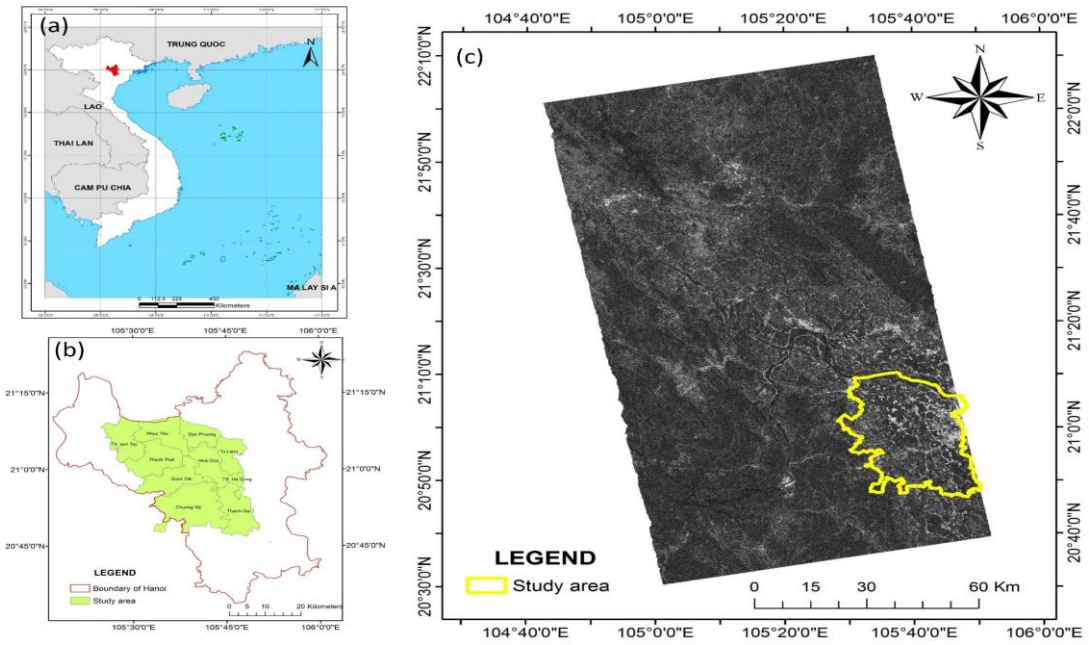

Fig. 1. (a) Location of Hanoi; (b) Location of study area in Hanoi;
(c) Study area in the coherence image of VV polarization.

3. Methodology

3.1. SAR coherence and the coherence of urban areas

Coherence was determined by the Interferometric synthetic aperture radar (InSAR) technique. The InSAR technique exploits the phase difference of two complex SAR images acquired from two orbit positions or different times [22]. The InSAR technique's complex SAR signal phase information is used for interferometric products, coherence images and permits measurements of change between two images. Different types of noise influence the accuracy of interferometric SAR images: atmospheric conditions such as humidity, temperature, and pressure, and changes in scatters. Perpendicular baselines and volume scattering create additional noise. Therefore, these noises also affect the coherence of the phase signals [23]. Coherence is a measurement of the degree of similarity between two waves. Thus, low coherence means that two wave patterns are not well correlated. In contrast, high coherence means highly correlated with two wave patterns [24]. The phase difference tells us more about geometry than random fluctuation due to noise. Local coherence is defined as the amplitude of the complex correlation coefficient between two SAR images [25] and is shown by Eq. (1) below:

$$\gamma = \left| \frac{\frac{1}{N}\sum_{i=0}^{N} M_i S_i^*}{\sqrt{\frac{1}{N}\sum_{i=0}^{N} M_i M_i^* \frac{1}{N}\sum_{i=0}^{N} S_i S_i^*}} \right| \quad (1)$$

Where N the number of neighboring pixels to be estimated; M and S are the complex master and slave image, and * denotes the complex conjugate [26].

The local coherence is estimated at a small window (a few pixels in range and azimuth) after the compensation of the terrain's effect. The coherence map of the scene is the result of a moving window that covers the whole SAR

image [23]. Multilooking can be performed to reduce noise.

The coherence value ranges from 0 (the interferometric phase is just noise) to 1 (absolutely absence of phase noise). The coherence is nearly 1, which means the observations are stable objects like buildings in the two images.

Land-cover includes vegetation, open water, and barren land (bare soil, urban). The difference roughness of surface and material properties changes backscatter and phase values on the SAR image. Interferometric correlation depends on the sensor (wavelength, signal-to-noise ratio, range resolution, number of independent looks), and geometrical parameters (baseline, incidence angle). Besides, volume scattering and the characteristic changes over time, such as wind, the humidity of the soil, temperature, growth, also decrease the coherence value of two images. Vegetation subjects often have a low degree of interferometric correlation due to volume scattering and plant growth. Coherence has been proved to help classify forests and urban areas [10]. Due to the effect of "specular reflection," the SAR image's water object has a low backscatter value and is distinguished from other land-cover features.

Moreover, the open water class's coherence value is low because of the low backscattering value in a pair of SAR images. Urban areas have a high backscatter value on the SAR image and a high coherence value. (Usai, S., 2000) [27] showed that human-made features such as cities and roads had a high coherence value in the image at two different times. The coherence value of urban areas has a threshold of 0.5 to 0.8 [27]. In the multi-temporal SAR images, the urban areas have stable backscatter value and coherence greater than 0.5 [8].

3.2. Workflow

The process consists of three main parts, including:

i) Creating the coherence image by using a pair of SAR interference images.

ii) Processing coherence image by computing multi-look and geometric correction to UTM coordinate system.

iii) Classification of the coherence image to urban/non-urban areas by optimal total threshold method.

The workflow chart is shown in Fig. 2.

The input image data is a pair of interferometric images with an SLC level with VV and VH dual polarization. The input data will be corrected terrain effects by DEM 1-sec SRTM data before computing coherence values.

In the next step, the input data need to deburst by TOPSAR deburst module. Then the coherence image needs to be multi-look calculated. In the article, the number looks are four. After that, the processed image was geometrically corrected to UTM coordinate system in which the Nearest neighbor algorithm for resampling; DEM with SRTM 1sec.

As a third step, the coherence image is classified into urban/non-urban layers. The total threshold method means using a single value (threshold) for all pixels in the image to convert to a binary image. This method is used for the images that are taken with the same lighting conditions. Coherence images are intensity images with range values from 0 to 1, in which urban areas are values ranging from 0.5 to 1.0. Hence, urban/non-urban areas are using the optimal total threshold method. The coherence image is classified as a binary image with an urban 1 value and non-urban at 0 value.

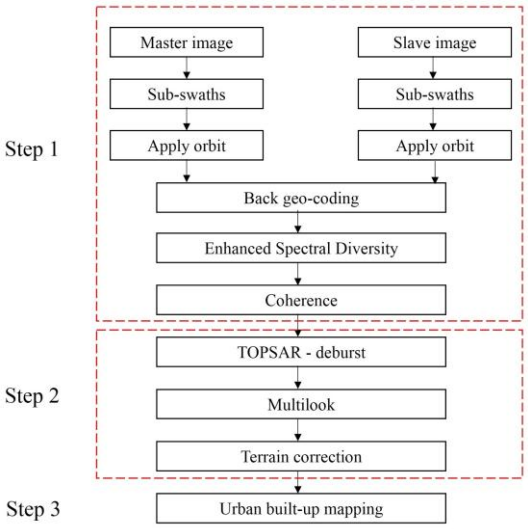

Fig. 2. The workflow chart for mapping urban areas.

3. Results and discussion

The authors experimented with processing the sub-swaths IW2 of a pair of Sentinel-1A images. The study area is Hanoi's central city (Fig. 1b), with a high population density, so the coherence image was cut based on the study area boundary (Fig. 3). The coherence image has a spatial resolution of 15m, the UTM coordinate system with zone 48. The SNAP toolbox processes the experience of Sentinel-1 data and is shown in Fig. 2. The coherence value of this image ranges from 0 to 1. The materials data consists of a pair of SAR interference images with a small perpendicular baseline. Besides, the period for acquiring two images was 12 days, so Hanoi's central residential area did not have a significant change. The coherence image's urban areas were interpreted visually based on the Sentinel-2A image (Fig. 4). The coherence value of the urban areas is high from 0.5 to 0.99.

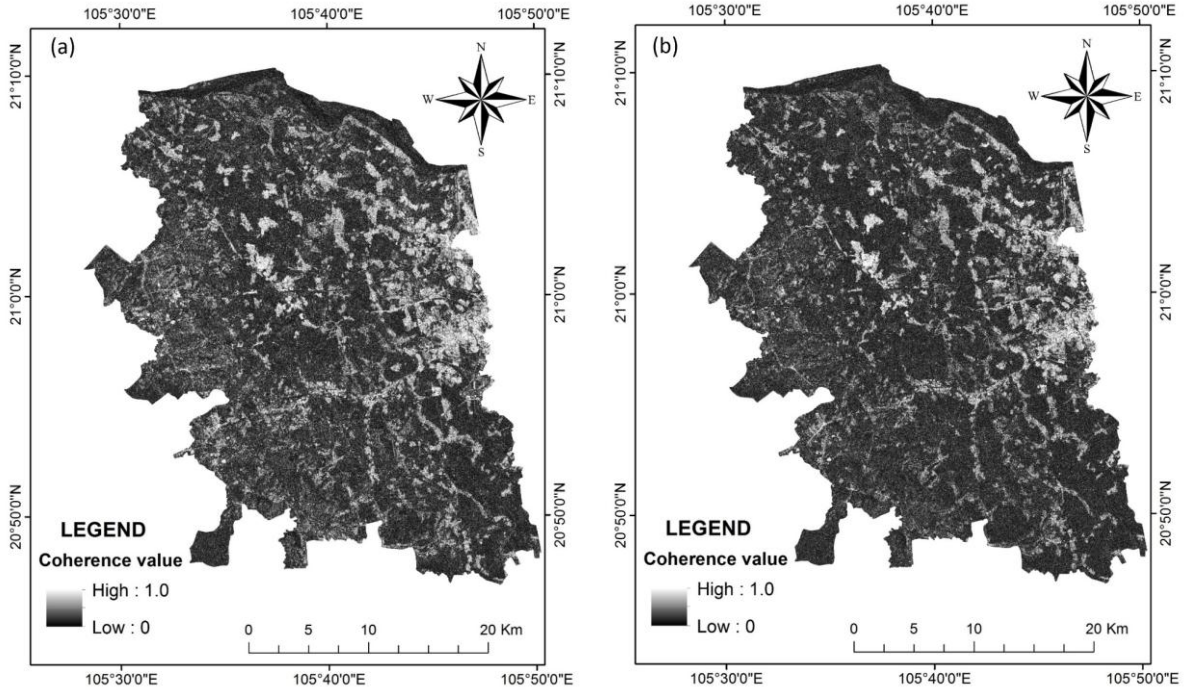

Fig. 3. The coherence image in the study area. (a) Coherence of VV polarization image; (b) Coherence of VH polarization image.

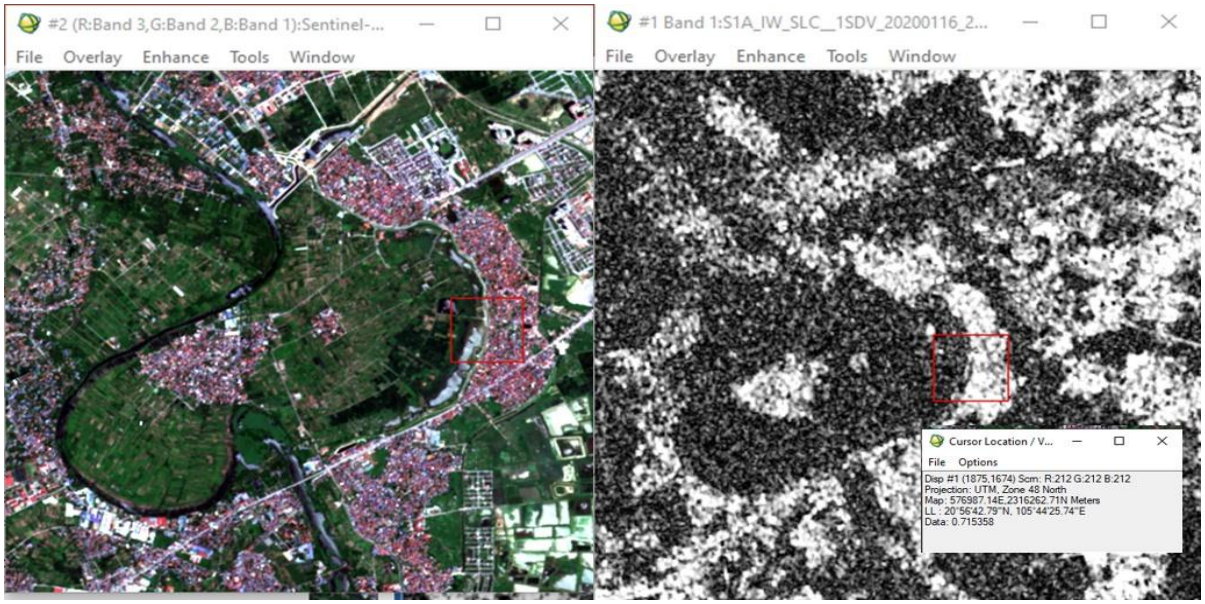

Fig 4. Defining threshold of urban areas on coherence image. (Left image) the natural color component of Sentinel-2A with Band4:Band3:Band2; (Right image) The coherence image.

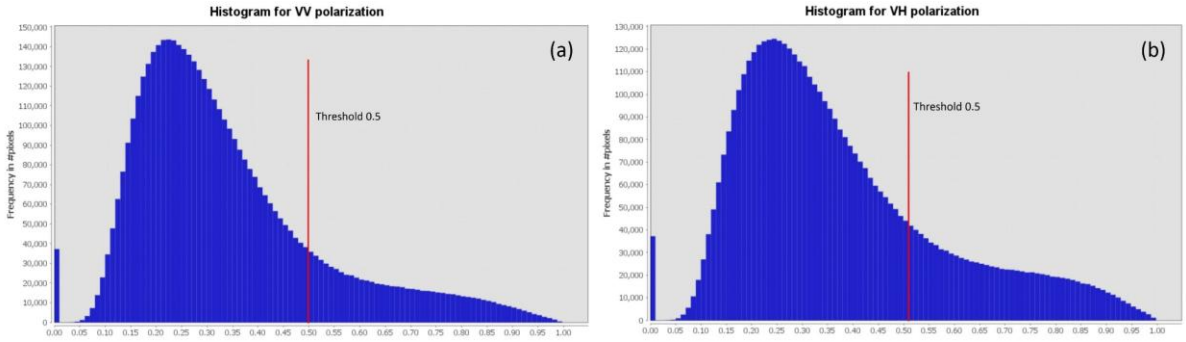

Fig 5. The histogram of the coherence images. (a) Histogram of VV polarization; (b) Histogram of VH polarization.

There are currently many automatic selecting optimal thresholds on images such as the Otsu, Huang method. However, the coherence image has speckle noise, so selecting the global threshold is still a disadvantage. According to the land-cover classification studies' analysis using coherence images, the urban feature has values from 0.5 to 0.9 [8, 27]. Based on the reference of urban areas on the Sentinel-2A image, the authors have defined urban areas' threshold value ranging from 0.5 to 0.99. Fig. 4 shows the natural color component of the Sentinel-2A and the coherence image at the same position.

Besides, the histogram of VV and VH graphs are nearly the same (Fig. 5). The position of threshold 0.5 at the histogram is located at the position of changes in pixel value distribution, so the threshold of 0.5 is suitable. Simultaneously, according to InSAR theory, the objects with a coherence value greater than 0.5 are called correlation on a pair of SAR interference images.

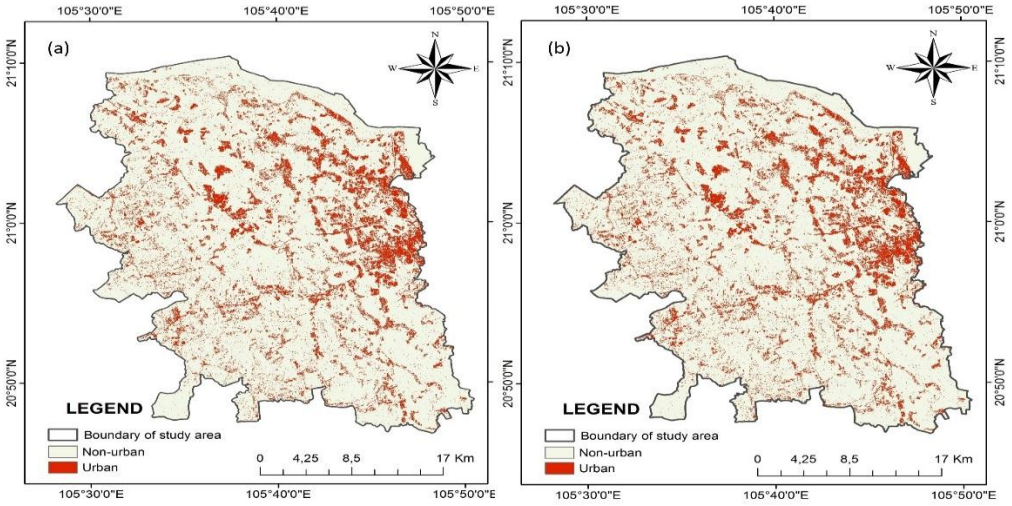

Fig 6. The classification images. (a) VV polarization image; (b) VH polarization image.

Therefore, the authors choose the threshold 0.5 for testing urban feature classification on the coherence image. The classification images included in the VV polarization (Fig. 6a) and VH polarization (Fig. 6b) in which urban is 1 value and non-urban is 0 value.

To evaluate classification accuracy, we used 100 random validation points extracted from high-resolution satellite imagery on Google Earth (Fig. 7a). The accuracy classification assessment with VV and VH polarization images is shown in Table 2 and Table 3.

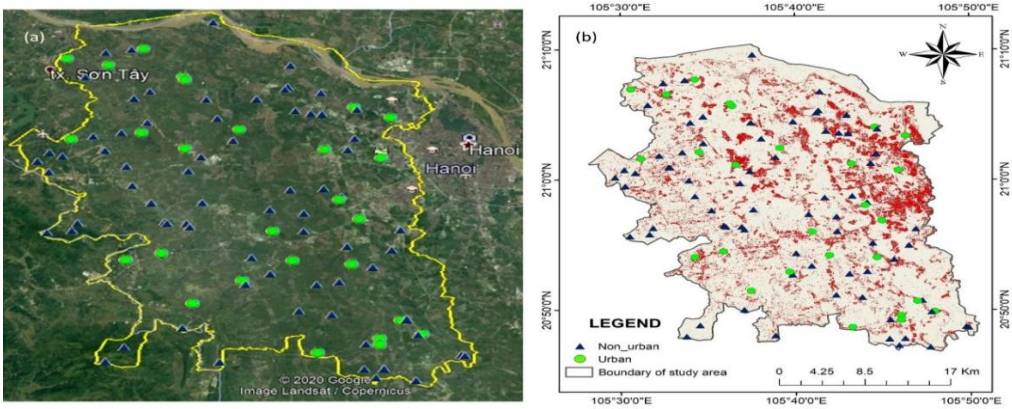

Fig 7. Evaluate classification accuracy using validation points.

Table 2. The assessment of classification with VV polarization image

Classification of VV polarization	Reference data (Google Earth)			
		Urban	Non-Urban	UA%
	Urban	15	08	65.2
	Non-Urban	03	74	96.1
	PA%	83.3	90.2	
Overall accuracy		89%		
Kappa index		0.6638		

Table 3. The assessment of classification with VH polarization image

Classification of VV polarization	Reference data (Google Earth)			
		Urban	Non-Urban	UA%
	Urban	18	07	72.0
	Non-Urban	0	75	100
	PA%	100	91.5	
Overall accuracy		93%		
Kappa index		0.794		

According to the results shown in Tables 2 and Table 3, the classifying accuracy of urban areas using coherence images achieved over 89%. In which the classification accuracy of VH polarized images is higher than on VV polarized images. It proves that the urban areas are classified well by the InSAR technique's coherence analysis on the Sentinel-1 images, especially in VH polarization. Unfortunately, the built-up features, such as barren land and road features, are not classified in this method. The barren land and roads have low backscatter value and are small in size on the Sentinel-1 image, especially in Hanoi's central, so that the coherence value is lower than 0.5.

5. Conclusion

In conclusion, the Sentinel-1A images with C-band and SLC level is suitable for determining the coherence image based on the InSAR technique. The pair of Sentinel-1 images has a small perpendicular baseline and a period of 12 days. Building features have a high coherence value from 0.5 to 0.9. The coherence characteristic is suitable for classifying building features but cannot classify barren land and roads due to low coherence value and low backscatter value on a pair of SAR interference images. The classification accuracy is over 89%, in which the classification of VH polarization images gives higher accuracy than those classified on VV polarization images. In the future, the authors will study the combine the coherence image and backscatter values with improving the classification accuracy of landcover features using SAR images.

Acknowledgments

Sentinel-1A images were provided by European Aerospace Agency (ESA).

References

[1] B. Bhatta, Quantifying the degree-of-freedom, degreeof-sprawl, and degree-of-goodness of urban growth from remote sensing data, Applied Geography, 30 (2010), 96–111. https://doi.org/10.1016/j.apgeog.2009.08.001.

[2] C. Sun, Z. Wu, Z. Lv, N. Yao, J. Wei, Quantifying different types of urban growth and the change dynamic in Guangzhou using multi-temporal remote sensing data, International Journal of Applied Earth Observation and Geoinformation, 21 (2013) 409-417. https://doi.org/10.1016/j.jag.2011.12.012

[3] A. R. As-syakur, W. S. Adnyana, W. Arthana, W. Nuarsa, Enhanced Built-Up and Bareness Index (EBBI) for Mapping Built-Up and Bare Land in an Urban Area, Remote Sensing, 4 (2012), 2957-2970. https://doi:10.3390/rs4102957.

[4] C. He, P. Shi, D. Xie, Y. Zhao, Improving the normalized difference built-up index to map urban built-up areas using a semiautomatic segmentation approach, Remote Sensing Letters, 1 (2010) 213-221. https://doi.org/10.1080/01431161.2010.481681.

[5] H. Xu, A new index for delineating built-up land features in satellite imagery, International Journal of Remote Sensing, 29 (2008), 4269-4276, http://dx.doi.org/10.1080/01431160802039957

[6] Y. Zha, J. Gao, S. Ni, Use of normalized difference built-up index in automatically mapping urban areas from TM imagery, International Journal of Remote Sensing, 24 (2003) 583-594. http://dx.doi.org/10.1080/01431160304987.

[7] H. Zhao, X. Chen, Use of Normalized Difference Bareness Index in Quickly Mapping Bare Areas from TM/ETM+, International Geoscience and Remote Sensing Symposium (IGARSS) 3 (2005)

1666 – 1668, http://10.1109/IGARSS.2005.1526319.

[8] C. Corbane, G. Lemoine, M. Pesaresi, T. Kemper, F. Sabo, S. Ferri, V. Syrris, Enhanced automatic detection of human settlements using Sentinel-1 interferometric coherence, International Journal of Remote Sensing, 39 (2017) 842-853. https://doi.org/10.1080/01431161.2017.1392642.

[9] F. Vicente-Guijalba, J. Duro, C. Notarnicola, A. Jacob, R. Sonnenschein, J.J. Mallorquí, C. López-Martínez, J.M. Lopez-Sanchez, Assessing hypertemporal Sentinel-1 coherence maps for land cover monitoring, In Proceedings of the 9th International Workshop on the Analysis of Multitemporal Remote Sensing Images (MultiTemp), IEEE, Belgium, 2017, https://doi: 10.1109/Multi-Temp.2017.8035240.

[10] L. Bruzzone, M. Marconcini, U. Wegmuller, A. Wiesmann, An Advanced System for the Automatic Classification of Multitemporal SAR Images, IEEE Transactions on Geoscience and Remote Sensing, 42 (2004) 1321–1334, https://doi: 10.1109/TGRS.2004.826821.

[11] M. Chini, R. Pelich, R. Hostache, P. Matgen, Built-up areas mapping at global scale based on adapative parametric thresholding of Sentinel-1 intensity & coherence time series, In Proceedings of the 9th International Workshop on the Analysis of Multitemporal Remote Sensing Images (MultiTemp), IEEE, Belgium, 2017, https://doi: 10.1109/Multi-Temp.2017.8035258.

[12] P. Washaya, T. Balz, B. Mohamadi, Coherence Change-Detection with Sentinel-1 for Natural and Anthropogenic Disaster Monitoring in Urban Areas, Remote Sensing, 10 (2018) 1-22. https://doi.org/10.3390/rs10071026.

[13] T.L. Hung, Urban Bare Land Classification Using NDBaI Index Based on Combination of Sentinel 2 MSI and Landsat 8 Multiresolution Images, VNU Journal of Science: Earth and Environmental Sciences, 36 (2020) 68-78 (in Vietnamese). https://doi.org/10.25073/2588-1094/vnuees.4537.

[14] N.H.K. Linh, Automatic creation of urban land distribution maps using IBI index from Landsat TM image: Case study in Hue city, Thua Thien Hue Province, GIS conference, (2011) 205-212 (in Vietnamese).

[15] N.T. Hien, Evaluate the accuracy of extracting construction land and bare land in urban areas from remote sensing images by index images, experiment in Hanoi, Master thesis, Hanoi University of Natural Resources and Environment, Hanoi, 2018 (in Vietnamese).

[16] N.B. Duy, Studying on the Interferometry SAR (InSAR) technique for Digital Elevation Model (DEM) generation using Open source Software NEST and SNAPHU, Can Tho University Journal of Science, 36 (2015) 77-87 (in Vietnamese).

[17] D.V. Khac, N.C. Kien, D.M. Tam, Applying RADAR interference method to determine land subsidence in the urban center of Hanoi city, Journal of Science and Technology in Civil Engineering, 2 (2015) 61-68 (in Vietnamese).

[18] L.V. Trung, H.T.M. Dinh, Measuring ground subsidence in Ho Chi Minh city using differential InSAR techniques, Science and Technology Development Journal, 11 (2008) 121-130 (in Vietnamese).

[19] K. Clauss, M. Ottinger, P. Leinenkugel, C. Kuenzer, Estimating rice production in the Mekong Delta, Vietnam, utilizing time series of Sentinel-1 SAR data, International Journal of Applied Earth Observation and Geoinformation, 73 (2018) 574-585. https://doi.org/10.1016/j.jag.2018.07.022.

[20] H. P. Phung, L. D. Nguyen, N. H. Thong, L. T. Thuy, A. A. Apan, Monitoring rice growth status in the Mekong Delta, Vietnam using multitemporal Sentinel-1 data, Journal of Applied Remote Sensing, 14 (2020) 1-23. https://doi.org/10.1117/1.JRS Sentinel-1.

[21] L.M. Hang, V.V. Truong, N.D. Duong, T.A. Tuan, Mapping land cover using multi-temporal sentinel-1a data: A case study in Hanoi, Vietnam Journal of Earth Sciences, 39 (2017) 345-359. https://doi.org/10.15625/0866-7187/39/4/10730.

[22] R. Bamler, P. Hartl, Synthetic Aperture Radar Interferometry, Inverse Problems, 14 (1998) 1-54.

[23] A. Ferretti, A. Monti-Guarnieri, C. Prati, F. Rocca, InSAR Principles: Guidelines for SAR Interferometry Processing and Interpretation, TM-19, ESA Publications, The Netherlands, 2007.

[24] I.H. Woodhouse, Introduction to Microwave Remote Sensing, Taylor and Francis, USA, 2005.

[25] C. Lopez-Martinez, X. Fabregas, E. Pottier, A new Alternative for SAR Imagery Coherence Estimation, In Proceedings of the 5th European Conference on Synthetic Aperture Radar (EUSAR'04), Germany, 2004.

[26] B. Kampes, S. Usai, In Doris: The delft object-oriented radar interferometric software, In Proceedings of the 2nd International Symposium on Operationalization of Remote Sensing, Deft University of Technology, The Netherlands, 1999.

[27] S. Usai, An Analysis of the Interferometric Characteristics of Anthropogenic Features, IEEE TRANSACTIONS ON GEOSCIENCE AND REMOTE SENSING, 38 (2000) 1192-1197. https://doi.org/10.1109/36.843050.